Exploring How Vitrimer Like Properties can be Achieved from Dissociative Exchange in Anilinium Salts

Progyateg Chakma,[†] Colleen N. Morley,[†] Jessica L. Sparks, [§] and Dominik Konkolewicz*[†]

†Department of Chemistry and Biochemistry, Miami University, Oxford, Ohio 45056, United States

§ Department of Chemical, Paper and Biomedical Engineering, Miami University, Oxford, Ohio 45056, United States

* Corresponding author: <u>d.konkolewicz@miamiOH.edu</u>

KEYWORDS. Dynamic covalent chemistry, Covalent adaptable networks, Vitrimer, Quaternary anilinium salts.

ABSTRACT: Dynamic covalent materials have properties such as self-healing, recyclability, and stress relaxation due to the dynamic exchange in the polymer networks. Here, an elaborate study on the kinetic exchange in anilinium salts and viscoelastic properties of dynamic covalent networks with anilinium linkages are studied. Mechanistic studies show that dynamic exchange in anilinium salts follow a *dissociative* pathway. Small molecule kinetics study suggests that despite the dissociative mechanism, there is an essentially constant molar composition or bond density across a wide temperature profile. Rheological studies indicate that covalent adaptable networks (CANs) with anilinium linkages provide viscoelastic properties similar to CANs with associative exchange processes networks. Additionally, thermal and microwave responsive self-healing and malleability

properties can be achieved in this network, along with the materials showing excellent creep resistance and creep recovery.

Introduction

Bonds that can undergo reversible cleavage and reformation have gained significant interest in polymer networks. Polymeric materials with dynamic linkages can show thermosets like superior mechanical properties along with thermoplastic like reprocess and recycleability. The dynamic nature of these bonds can introduce unique properties such as self-healing, stress relaxation, degradability, malleability, shape-memory, and adaptability in materials.¹⁻⁹ These dynamic polymer networks are either based on dynamic supramolecular interactions or dynamic covalent bonds (DCBs).² Polymeric materials based on DCBs are often coined as covalent adaptable networks (CANs), which are static under ambient conditions.¹⁰ However, the reversible nature of DCBs can be activated in response to stimuli such as light, pH, and temperature.¹¹⁻²¹ This leads to polymer networks with excellent mechanical properties and stability along with on demand dynamic properties under different environmental conditions.^{10,22}

Dynamic exchange in DCBs can occur either via a dissociative or an associative mechanism.^{5,10,23} The Diels-Alder (DA) reaction is a classic example of DCBs that follows the dissociative mechanism.^{24,25} At elevated temperatures the DA linkages completely dissociate first via retro-DA and then reform after some time at lower temperatures (Scheme 1). In macromolecular networks this results in a sudden change in network structure due to complete dissociation of crosslinkages when dynamic covalent linkages are activated.^{26,27} Reactions like transesterification (TE) on the other hand, follow an associative exchange mechanism, where dynamic covalent bonds break and reform simultaneously (Scheme 1)²⁸. As a result, material's mechanical integrity can be retained by having a permanent crosslinkers density at all the times. Materials with associative DCBs have

been coined as 'vitrimers', where viscosity of the materials is controlled by thermally induced chemical exchange in the networks.²⁹ So far, a plethora of covalent reactions have been used in developing vitrimeric materials.²⁹⁻⁴⁴

A) Dissociative DCB: reverible Diels-Alder reaction

B) Associative DCB: Transesterification

$$R_1$$
 R_2 R_3 R_3 R_4 R_3 R_4 R_5 R_6 R_7 R_8 R_8 R_9 R_8 R_9 R_9

C) This work - indirect S_N2 exchange in Anilinium Salts

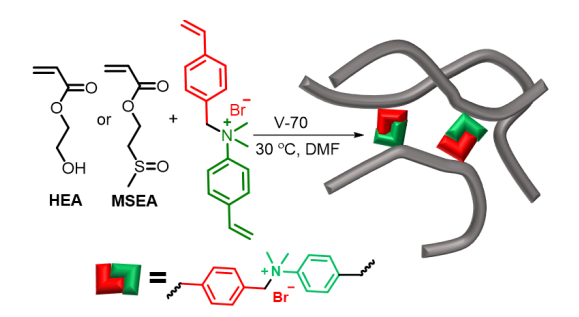
- Dissociative DCB acts like associative DCB in polymer matrix

Scheme 1. A) reversible DA reaction of furan and maleimide, B) Thermally activated TE reaction C) dissociative dynamic exchange in anilinium salts

Recently, our group has reported the small molecular kinetics of the dynamic exchange in quaternary anilinium salts at elevated temperature and its utilization in dynamic materials.⁴⁵ The dynamic exchange in anilinium salts, which occurs through bimolecular nucleophilic substitution (S_N2), can be activated in response to mild thermal stimulus (60 °C) and it follows a dissociative mechanism via indirect or non-concerted S_N2 pathway (Scheme 1). Previously, Kulchat and Lehn also reported similar results.⁴⁶ Recent reports also suggests that some dissociative DCBs can have 'vitrimer' like properties with either fast bond reformation or very high equilibrium constants in favor of the bonded state.⁴⁷⁻⁵¹ Despite these few reports, an extensive study on small molecular kinetics of exchange in these types dissociative DCBs has not been well explored. To be noted a thorough study of how fast dissociative urethane exchange leads to vitrimer like materials were

recently reported by Hillmyer and coworkers, however products of the dissociation of urethane weren't observed.⁵¹ In anilinium system, the products of the both forward and reverse reaction can be easily observed and leads to better understanding of the system. Additionally, a correlation between small molecular kinetics to flow behavior of macromolecular networks with these types of DCBs should be needed to discover how materials with DCBs can maintain relatively constant network properties expected of an associative CAN. This is very intriguing, since it has been argued that only associative DCBs induce 'vitrimeric' characteristics.³¹

In this report, we study why dissociative DCBs, using anilinium bonds as a model system, can create vitrimer-like CAN materials. The main focus was to correlate small molecule kinetics of dynamic exchange in anilinium salts to vitrimer-like flow behavior of polymeric materials with anilinium linkages. It was found that despite a dissociative exchange pathway, it is possible to retain an essentially constant crosslink density over a wide range of temperatures. Additionally, two distinct monomers were utilized to synthesize dynamic networks (Scheme 2), and the effects of the monomer's polarity and protic nature on the materials' dynamic properties were explored, in light of the underlying $S_{\rm N}2$ chemistry. The dynamic properties of these anilinium networks were compared to a control network made of DA linkages to highlight the unique features of the anilinium based dissociative networks.



Scheme 2. Synthesis of polymer networks with anilinium linkages by free radical polymerization.

Experimental Section

Materials. All reagents were obtained from commercial sources and used without any purification, unless mentioned otherwise.

Characterization methods. All ¹H nuclear magnetic resonance (¹H NMR) experiments were carried out in a Bruker 300 or 500 MHz spectrometer. All NMR kinetics data was processed in Bruker TopSpin 4.0.6 software. Infrared (IR) spectroscopy data was collected by using a Perkin Elmer Spectrum 100 Spectrometer. A TA instruments DSC Q2000 was used to obtain glass transition temperature (T_g) of each material. The data was obtained in a heat cool heat cycle ranging from - 40 °C to 160 °C with 10 °C per minute heating rate. The data was plotted only from the second heating cycle. All of the materials were completely dried before mechanical analysis.

Tensile testing. Uniaxial tensile testing experiments were carried out on dog bone shaped materials in an Instron 3344 universal testing system equipped with a 100 N load cell. The extension rate was 1 mm/s and data was collected until the material failed. All the experiments were performed in ambient condition. The peak stress and strain at break of uncut/virgin materials were obtained as the mean and standard deviations of at least 4 replicates. The Young's modulus (E) values of all the materials were obtained by modelling the tensile responses of the materials using the Ogden hyper elastic constitutive law (Equation 1)⁵²:

$$\sigma_{eng} = \frac{2G}{\alpha} \left[\lambda^{\alpha - 1} - \lambda^{-1 - (\alpha/2)} \right] \qquad (1)$$

where, σ_{eng} is the engineering stress, G is the shear modulus, α is the strain hardening exponent, and λ is the stretch ratio. The values of G and α were determined for each sample by fitting Eq. 1 into the experimental data obtained from tensile testing. The value for Young's modulus or elastic modulus (E) was calculated by using Equation 2:

E = 2G(1 + v) (2) Here, v is the Poisson's ratio with the value of 0.5 for an incompressible type material.

Rheology. The rheology experiments were carried out using a TA instrument Discovery HR-1 rheometer. A 20 mm crosshatched plate geometry were used for all the experiments. In all cases rheology disks were synthesized in a 20 mm diameter circular Teflon mold. Rheological frequency sweeps experiments were carried out from 10⁻³ to 10² Hz frequency at 1% applied strain at 25 °C. All strain sweep experiments were performed over the range of .01% strain to 10% strain with constant frequency of 1 Hz at 25 °C. All temperature sweep experiments were carried out from 4 °C to 195 °C at a heating rate of 5 °C min⁻¹, with an angular frequency of 6.28 rad/s and 1% strain. All the stress relaxation experiments were performed in a strain control (1% strain (within linear range)) at different temperatures. In all cases, the sample was allowed to relax at room temperature for 30 minutes to remove stress relaxation attributed to segmental movement in the network. Additionally, the sample was allowed to equilibrate at a particular temperature for 3 minutes before data was collected. In all cases, stress relaxation modulus was allowed to decay to at least 37% (1/e) of its initial modulus value. The Maxwell equation for viscoelastic materials was used to calculate the characteristic relaxation time as shown in Equation 3.³⁹

$$\frac{G_t}{G_0} = e^{\frac{-t}{\tau^*}} \tag{3}$$

Where, G_t is the relaxation modulus at time t, G_0 is initial relaxation modulus, τ^* is the characteristic stress relaxation time at $G_t/G_0 = 1/e$. In all cases, G_0 was measured from t = 60s to remove initial noisy data. τ^* values at different temperatures were then plotted in the Arrhenius equation to achieve the activation energies (Equation 4).

$$\ln \tau^* = \ln A + \frac{E_A}{RT} \tag{4}$$

Where, A is pre-exponential factor, E_A is activation energy, R is universal gas constant, T is temperature in Kelvin.

Healing. For healing experiments, dog bone shaped materials were cut into two sections using a razor blade and then placed in contact using fingers for a few seconds. The reattached dog bones were placed into a preheated oven at 70 °C for healing at different time periods. Healing experiments were carried out using a commercially available microwave oven (sharp carousel SMC2242DS 1200W). The experiments were replicated at least two times for each data point.

Malleability. Material was fixed into twisted 360° configuration using paper clips and then placed in a preheated oven at 70 °C. After certain period, material was removed from oven, clips were removed and then allowed to relax at ambient conditions for 7 days. The angle between the two ends of twisted material was measured to determine malleability properties. The experiment was replicated two times.

Creep and creep recovery. Creep and creep recovery experiments were performed in a TA instrument DMA Q800 equipped with a tension film clamp. In all the experiments, a stress of 50 kPa was maintained during the strain measurement for 2 h. After 2 h, the constant stress was removed, and the strain were measured over 2h time period. The creep recovery data was collected for 2 h.

Healing efficiency. Healing efficiency of the PHEA-VBABr and PMSEA-VBABr materials were measure by the following formula;

$$Healing \ efficiency \ (\%) = \frac{\text{Mechanical value of the healed material}}{\text{Mechanical value of the uncut material}} \times 100$$

Here, mechanical value refers to stress at break or strain at break.

Swelling ratio. Samples of PHEA-VBABr and PMSEA-VBABr materials were weighed and added into vials with excess amount of solvents. Swelled samples were taken out of vials, blotted, and then weighed. This process was repeated until equilibrium reached. The swelling ratio of the materials were measured by the ratio of the mass of the swelled sample to the mass of the sample before swelling.

Synthesis. Synthesis of N-Benzyl-N,N-dimethylbenzenaminium bromide (ABBr) and Synthesis of N-Benzyl-N,N,4-trimethylbenzenaminium bromide (MABBr).

Synthesis of ABBr and MABBr were carried out following our previous literature report. 45

Synthesis of 2-(Methylsulfinyl)ethyl Acrylate (MSEA). Synthesis of MSEA was carried out following the procedures from literature and the purity was confirmed by ¹H-NMR.^{53,54}

Synthesis of 4-(N,N-Dimethylamino)styrene (AS). Synthesis of AS was carried out following previously reported procedure and confirmed by ¹H-NMR.^{45,55}

Synthesis of 4-Vinyl benzyl bromide (VBBr)

Synthesis of VBBr was carried out following previous literature report and confirmed by ¹H-NMR.^{45,56}

Synthesis of N,N-dimethyl-4-vinyl-N-(4-vinylbenzyl)benzenaminium bromide (VBABr).

Synthesis of AS was carried out following previous literature report and confirmed by ¹H-NMR.⁴⁵

General procedure for synthesis of PHEA-VBABr and PMSEA-VBABr Networks.

2-Hydroxyethyl acrylate (HEA) (4g), **2,2'-Azobis(4-methoxy-2,4-dimethylvaleronitrile)** (V-70, 40 mg), N,N- dimethylformamide (DMF) (8ml), VBABr crosslinker (0.120g and 0.200g) were added into vials for PHEA-3%VBABr and PHEA-5%VBABr materials respectively. The solution mixture was then ultra-sonicated for 15 minutes for proper mixing and then transferred to a pre-

heated Teflon mold. The polymerization was carried out at 30 °C for 3h. After 3 h, dog bone shaped crosslinked materials were removed from the Teflon mold. Typically, a conversion of approximately 95% was achieved, that was confirmed by gravimetric method. The materials were allowed to dry for 2 days inside hood, followed by another 2 days in a vacuum oven at 30 °C to remove solvent from the network. PMSEA-VBABr materials were also synthesized following the same procedure. Additionally, PMSEA-VBABr-AS networks were also synthesized following same procedure, where 1 molar equivalent of free AS to VBABr crosslinker was added. Removal of excess solvent was confirmed by IR spectrum. Circular shaped rheology disks were also synthesized following the same procedure.

General procedure for synthesis of PEA-DA networks.

Ethyl acrylate (EA) (6g), 2,2'-azobis(2-methylpropionitrile) (0.06g), furfuryl methacrylate (.5g), 1-dodecanethiol (0.365 g), and toluene (8g) were added into a 50 mL round bottom flask equipped with a stirrer bar. The reaction mixture was then capped with a rubber septum and then deoxygenated for 30 minutes. The reaction was stirred for overnight at 65 °C. A conversion of 90% was achieved and PEA-DA polymer was recovered by precipitating in hexane. Finally, PEA-DA polymer (4g) was mixed with 0.55 molar amount of 1,1'-(methylenedi-4,1-phenyl-ene bismaleimide and 8g of DMF and the mixer was transferred to Teflon mold for network formation at 50 °C for overnight. Once crosslinked, the circular shaped rheology disks were removed from Teflon mold and allowed to dry for 2 days inside hood, followed by another 2 days in a vacuum oven at 30 °C to remove solvent from the network.

Kinetic study of anilinium salts dissociation.

In a vial, ABBr adduct (0.2036 g, 0.000696 mol) and 5 g of HPLC grade acetonitrile were added and stirred until all the components were dissolved. From this stock solution, 2 mL of mixture was

transferred to small vials, capped with rubber septum, and then heated at different temperatures (55 °C, 60 °C, 65 °C) in an oil bath. 0.1 mL sample was taken at different time points and added to CDCl3 for NMR analysis. Kinetic study of MABBr dissociation was carried out following the same procedure.

Kinetic study of anilinium salts and free tertiary amines exchange.

In a vial, ABBr adduct (0.2036 g, 0.000696 mol) and MA (.09412 g, .000696 mol) were added to 5.2 g of HPLC grade acetonitrile. The mixture was stirred until a clear solution was achieved. From that stock solution, 2 mL of mixture was transferred to into small vials, capped with rubber septum, and then heated at different temperatures (50°C, 55 °C, 60 °C, 65 °C, 70 °C) in an oil bath. From the vial, 0.1 mL sample was taken at different time points and added to CDCl3 for NMR analysis. The exchange between MABBr and A were carried out following the same procedure.

Results and Discussions

Solubility Experiments. Polymeric networks of 2-hydroxyethyl acrylate (HEA) or 2-(methylsulfinyl)ethyl acrylate (MSEA), crosslinked with an anilinium salts based crosslinker N,N-dimethyl-4-vinyl-N-(4- vinylbenzyl) benzenaminium bromide (VBABr) were synthesized using conventional radical polymerization. Initially, swelling behavior of these networks at elevated temperature were tested. If these materials behaved like traditional dissociative networks, they should dissolve in solvent at elevated temperature due to complete dissociation of the crosslinkages driven by entropy and dilution.³⁹ We observed both PHEA VBABr and PMSEA-VBABr networks only swelled but did not dissolve in excess DMF (150 °C, 48 h) (Figure 1A). However, when materials were allowed to swell in excess aminoethanol and potassium iodide, they were completely dissolved in 48 h at 150 °C (Figure 1B). This temperature is 90 °C higher than the temperature needed to activate the dynamic exchange in anilinium linkages.^{45,57} This suggests that

although the mechanism of exchange in the anilinium linkages is dissociative, possibly due to rapid dissociation-reassociation mechanism, they act similar to associative systems by retaining the crosslinking points in the polymer networks. Similar results were observed when experiments were performed using DMSO. Control experiment were carried out on Poly ethyl acrylate materials with Diels-Alder (PEA-DA) crosslinkages. PEA-DA networks were synthesized, which have furanmaleimide based DA linkages as shown in scheme 3. As shown in Figure S1, PEA-DA networks completely dissolved in hot DMF (110 °C, 2 h) due to complete dissociation of the furanmaleimide DA linkages. The furan maleimide based DA adducts typically dissociate at above 100 °C. This indicates a different thermodynamic behavior in the anilinium system compared to traditional dissociative DCBs like the reversible DA reaction. In order to understand how a dissociative anilinium system acts like an associative in CAN it is necessary to study small molecule kinetic study for exchanges over a range of temperature.

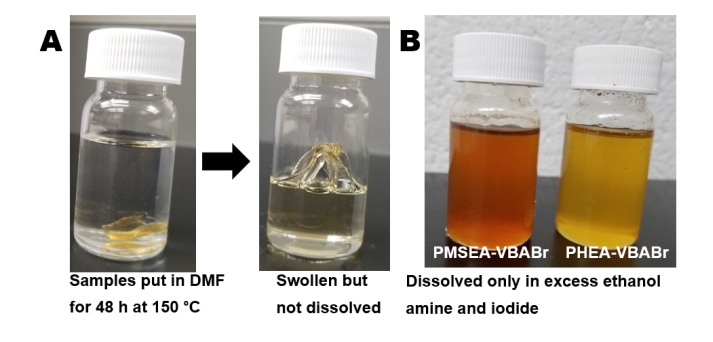


Figure 1. Solubility test – A) PMSEA-VBABr network only swells but does not dissolve in hot DMF B) polymer networks with anilinium linkages dissolved in excess free amine and halide.



Scheme 3. Synthesis of PEA-DA networks by post-polymerization cross-linking of furan and maleimide.

Small Molecule Kinetics. Small molecule kinetic experiments were performed on model compounds to study reversible exchange and molar concentration of different species over a range of temperatures. We studied dissociation of isolated quaternary anilinium salts, to monitor the equilibrium between associated salt, dissociated anilines, and benzyl bromide. Additionally, the exchange in composite systems i.e. the exchange between anilinium salts and free amine at elevated temperatures of 55 °C, 60 °C, and 65 °C in acetonitrile were also studied.

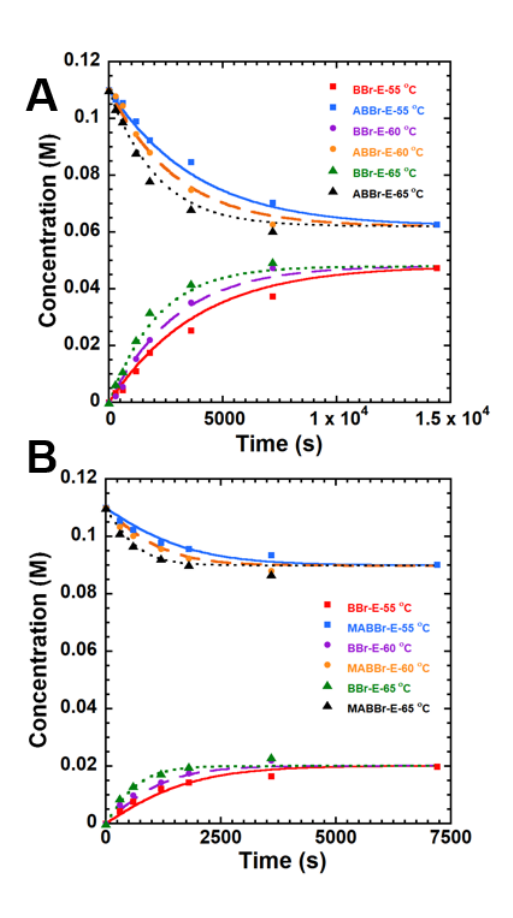


Figure 2. A) Equilibration of ABBr with BBr and B) Equilibration of MABBr with BBr at different elevated temperatures. Here, experimental points are labelled as E, and curve lines are the theoretical fits generated from kinetic model. Details of the kinetic model can be found in SI.

N-Benzyl-N,N-dimethylbenzenaminium bromide (ABBr) and N-Benzyl-N,N,4trimethylbenzenaminium bromide (MABBr) were used as the anilinium salts, while aromatic tertiary amines (N,N-dimethylaniline (A) and N,N-dimethyl-p-toluidine (MA)) were used as the free tertiary amines for the kinetic study. The details of the kinetic experiments can be found in supporting information. Dissociation of ABBr and MABBr salts were studied at elevated temperatures. The stacked 1H NMR plots of these experiments were given in Figure S2-S15. Benzyl bromide (BBr) is formed by the attack of bromide anion at benzylic carbon of the ABBr salts via an indirect S_N2 mechanism as highlighted in Scheme 1C. At each temperature, the equilibrium concentration of ABBr and BBr are similar. However, reaction rate increases with the increase of temperature. A kinetic model was used to get the theoretical fits of these exchanges using MATLAB. In the kinetic model, direct S_N2 i.e. attack of free tertiary amine on benzylic carbon of the anilinium salt was assumed to be negligible, based on prior work.⁴⁵ Details of this model can be found in SI. Figure 2A shows the kinetics curves of experimental data (E series) and theoretical fits (T series).

Similarly, the dissociation of MABBr at elevated temperatures were studied. MABBr and BBr also have similar molar compositions at different temperatures, once the equilibrium was reached (Figure 2B). This suggests that an essentially constant molar density of anilinium linkages can be retained, at least in the studied elevated temperatures. The dynamic exchange between quaternary anilinium salts (ABBr and MABBr) and free tertiary aromatic amines (MA and A respectively) were also studied at elevated temperatures. Figure 2 shows the exchanges reached a common equilibrium in 2h, 4h, and 6h time periods at 60 °C.55 °C and 65 °C respectively. In all the cases, the exchange was observed by the relative ratio of benzylic protons at 4.2 to 5.3 ppm region. Interestingly, at each temperature, all the components had similar mole fractions at equilibrium,

although, with the increase of temperature, the exchange reached equilibrium faster. The kinetic model was used to derive the rate coefficients (k_{xa1}, k_{xa2}, k_{bx1}, and k_{bx2}) of the exchanges by fitting theoretical data to experimental data. In is important to note that, we used an equilibrium constant (K_{eq}) derived from the experimental data obtained kinetic study of dissociation of isolated ABBr and MABBr to describe the parameters k_{xa1}, k_{xa2}, k_{bx1}, and k_{bx2} in our model. The values of these parameters obtained from fitting theoretical data to experimental data of dissociation of ABBr and MABBr at different temperatures, then used in composite systems. Where, k_{xa1} and k_{xa2} are the rate coefficients for attack of Br anion on benzylic carbon of anilinium adduct ABBr and MABBr respectively, k_{bx1} and k_{bx2} are the rate constants for the attack of N,N-dimethylaniline (A) and N,N-dimethyl-p-toluidine (MA) on benzylic carbon of benzyl bromide to form ABBr and MABBr adducts respectively. Arrhenius plot was used to derive the activation energy of these exchanges by plotting the data obtained from 55 °C, 60 °C, and 65 °C, and also extrapolating to 50 °C and 70 °C. (Figure 3).

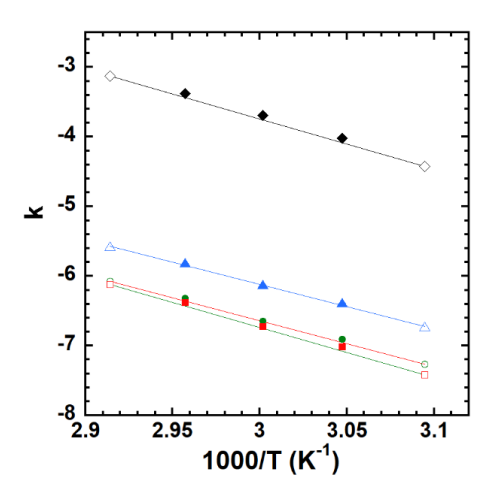


Figure 3. Arrhenius plots for all the rate coefficients - k_{xa1} (green), k_{xa2} (red), k_{bx1} (blue), and k_{bx2} (black). Solid points are based on experimental data and open points are based on extrapolated data.

Experimental data obtained from the kinetic of exchange of ABBr with MA at 50 °C and 70 °C were used to validate these extrapolations (Figure 4). It was found that the bromide attack on the benzylic carbon to dissociate C-N bond (k_{xa2}) is the rate determining step and the activation energy (E_a) was calculated to be 61 ± 1 kJ mol⁻¹ The E_a of the attack of free amine to the benzyl bromide (k_{bx2}) was calculated as 58 ± 2 kJ mol⁻¹. The similar E_a values imply that after dissociation of anilinium adduct, newly formed free amine can rapidly react with benzyl bromide to form a new anilinium adduct.

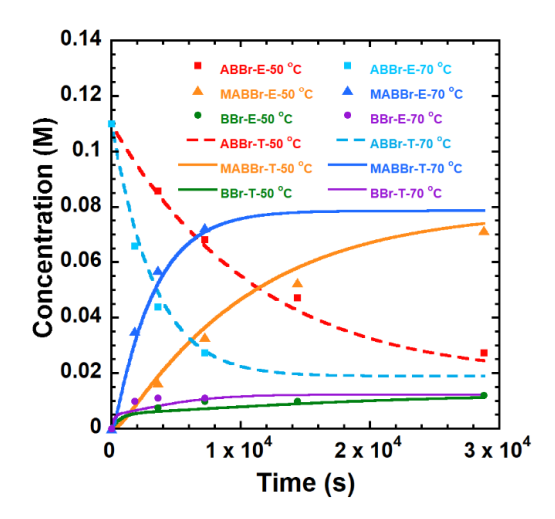


Figure 4. Kinetics of exchange between ABBr and MA at 50°C and 70°C. E series is based on experimental data obtained from ¹H-NMR experiments and T series are fitted theoretical fits from kinetic model.

Since the K_{eq} is the ratio of the rate coefficients, this suggests that the K_{eq} has minimal temperature dependence. These results suggest that under the studied conditions, despite the dissociative type exchange, an essentially constant crosslink density can be preserved in networks via a decrosslinking-recrosslinking mechanism at elevated temperatures. This is despite the fact that the Keq for adduct formation is relatively small at $K_{eq} = 3$ for ABBr formation and $K_{eq} = 20$ for MABBr

formation. Due to the same E_a value of both association and dissociation over a wide temperature range, it is indeed likely that constant crosslink density may be realized over a very wide temperature range. The equilibrium constant remains essentially constant over the studied temperatures, suggesting equilibrium favors the anilinium adduct, rather than to free aniline or benzyl bromide over this whole range of temperatures. Eyring-Polanyi analysis also gives a very similar plot to Arrhenius plot and similar values of enthalpy of activation (ΔH^{\ddagger}) to the E_a values obtained from Arrhenius analysis. Very small entropy of activation (ΔS^{\ddagger}) values imply trivial entropic contribution to the energy barrier. Calculated values of natural log of Arrhenius preexponential factor (lnA), $E_a \Delta H^{\ddagger}$, and ΔS^{\ddagger} are given in Table 1.

Table 1. calculated values of lnA, E_a , ΔH^{\ddagger} , and ΔS^{\ddagger}

Rate coefficients	lnA (Arrhenius)	E _a (Arrhenius)	$\Delta H^{\ddagger}(Eyring)$	ΔS^{\ddagger} (Eyring)
k _{xa1}	13.2± 0.7	54 ± 1 kJ mol ⁻¹	52 ± 1 kJ mol ⁻¹	0.08 ± 0.02 kJ K ⁻¹ mol ⁻¹
k_{xa2}	15.3± 0.3	61 ± 1 kJ mol ⁻¹	57 ± 2 kJ mol ⁻¹	0.09 ± 0.03 kJ K ⁻¹ mol ⁻¹
k_{bxi}	13.3± 0.5	53 ± 1 kJ mol ⁻¹	50 ± 1 kJ mol ⁻¹	0.08 ± .03 kJ K ⁻¹ mol ⁻¹
$k_{\rm bx2}$	18.1± 0.8	58 ± 2 kJ mol ⁻¹	57 ± 2 kJ mol ⁻¹	0.12 ± .03 kJ K ⁻¹ mol ⁻¹

Additionally, the Van 't Hoff analysis resulted in the enthalpy of formation (ΔH) and entropy of formation (ΔS) for the MABBr formation of -2.8 \pm 0.2 kJ mol⁻¹ and .0170 \pm .0005 kJ K⁻¹ mol⁻¹ respectively. This very small value of ΔH implies trivial dependence of Keq to temperature. On the other hand, ΔH and ΔS for the formation of ABBr were -15 \pm 1 kJ mol⁻¹ and - .0370 \pm .0004 kJ K⁻¹ mol⁻¹. The Van 't Hoff Plots are given in Figure 5.

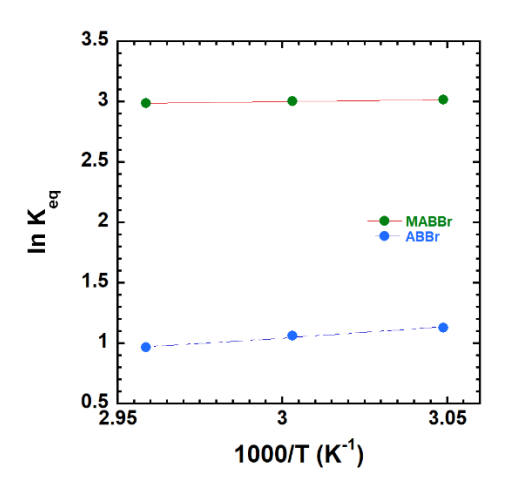


Figure 5. Van 't Hoff plots for equilibrium of dissociation of MABBr and ABBr.

Polymer Networks Synthesis and Characterizations. HEA and MSEA based networks PHEA-VBABr and PMSEA-VBABr were synthesized with 3 wt% and 5 wt% VBABr crosslinker using free radical polymerization. In addition, PMSEA-5%VBABr-AS materials were synthesized, where free aniline (AS) was incorporated in the network.

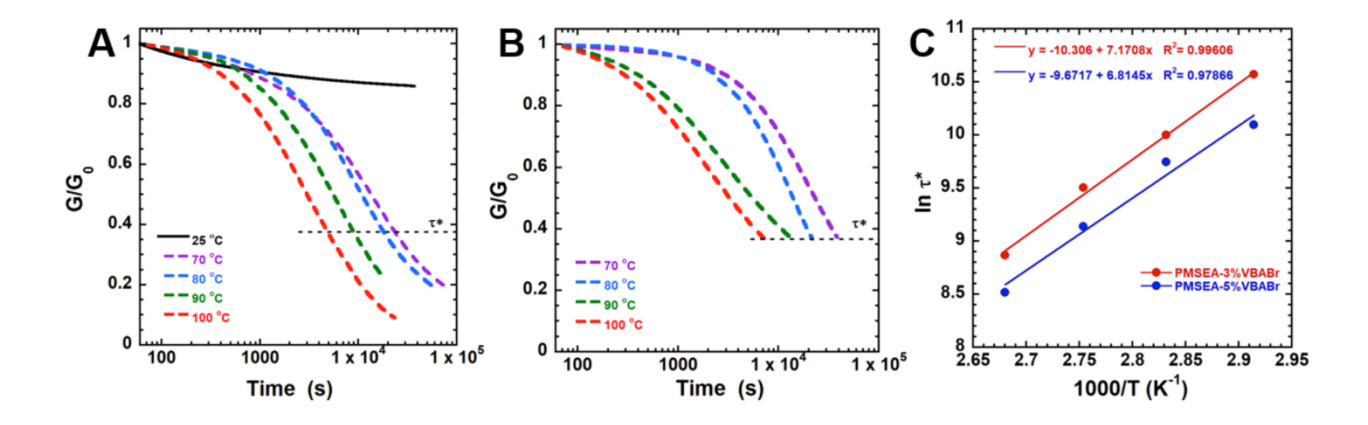


Figure 6. Representative stress relaxation plots of A) PMSEA-5%VBABr and B) PMSEA-3%VBABr materials at different temperatures. C) Representative Arrhenius plots of PMSEA-5%VBABr and PMSEA-3%VBABr materials.

Shear rheology of PHEA-VBABr and PMSEA-VBABr materials was performed to study the stress relaxation behavior and quantify the activation energies E_a of bond exchange and relaxation in these materials. In the literature, stress relaxation experiments have been utilized as a benchmark to characterize vitrimeric materials.³¹ Stress relaxation experiments were carried out on PMSEA-VBABr materials at 25 °C ,70 °C, 80 °C, 90 °C, and 100 °C and characteristic relaxation time (τ*) was calculated at 37% of the initial modulus values. In all cases, materials were allowed to relax at least 37% of the initial modulus. The stress relaxation plots of these materials are given in Figure 6A and 6B. As shown in Figure 6A, very negligible stress relaxation was observed at 25 °C, since anilinium linkages are essentially static at room temperature. Ea of the macroscopic flow in these networks by exchange in the crosslinkages were determined by plotting in the Arrhenius equation (Figure 6C). The E_a of PMSEA-5%VBABr and PMSEA-3%VBABr were calculated as 57 ± 5 kJmol⁻¹ and 60 ± 3 kJmol⁻¹ respectively. Similar E_a values in these networks indicates that the same exchange mechanism happens irrespective of molar compositions. These values are similar to the activation energy we obtained from the small molecule exchange experiments (61 ±1 kJ/mol).

Stress relaxation experiments were also carried out on PHEA-VBABr materials. Representative stress relaxation plots of PHEA-3%VBABr materials are given in Figure 7A and a comparison of stress relaxation with PMSEA-5%VBABr materials at 100 °C are given in Figure 7B. Figure 7B shows a significantly slower stress relaxation in PHEA-3%VBABr materials than in PMSEA-3%VBABr materials. A similar trend was found between PHEA-5%VBABr and PMSEA-5%VBABr materials. The stress relaxation plots of PHEA-5%VBABr materials can be found in Figure S16, where materials also only stress relaxed at elevated temperature and very miniscule stress relaxation was observed at room temperature. We assume, a solvation effect could be the

reason behind the faster relaxation in PMSEA-VBABr networks in comparison to PHEA-VBABr networks.

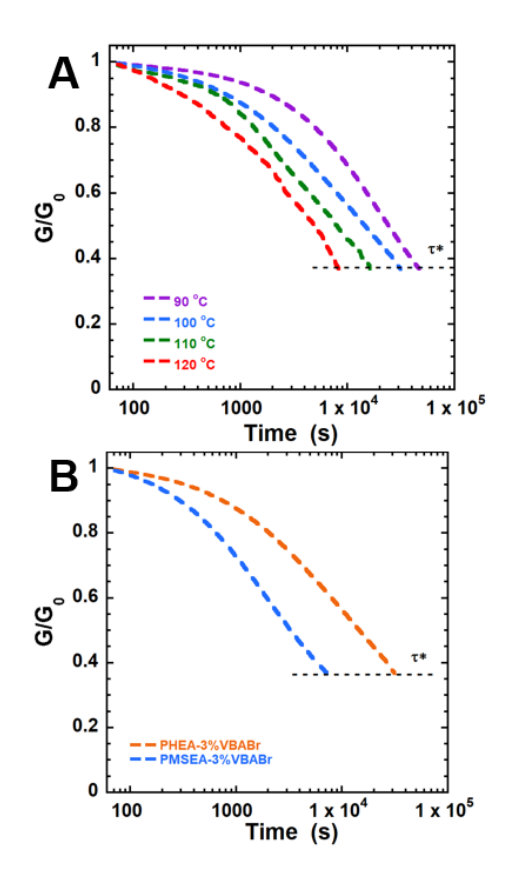


Figure 7. A) Representative stress relaxation plots of PHEA-3%VBABr materials B) Comparison of stress relaxation of PHEA-3%VBABr and PMSEA-3%VBABr materials at 100 °C.

The solvation effect in a S_N2 reaction is widely known.⁵⁹⁻⁶¹ S_N2 reactions are faster in polar aprotic solvents, as compared to polar protic solvents. MSEA has a polar aprotic type structure (similar to dimethyl sulfoxide)⁵³ that helps to dissolve ionic anilinium salts and make the anionic nucleophile bromide anions more available for nucleophilic attack by not solvating them. HEA on the other hand has a structure similar to a polar protic solvent (similar to ethanol) that slows down the S_N2 type attack of bromide anions in benzylic carbon of anilinium salt by solvating them. This is evident by the Ea of the exchange in PHEA-5%VABr and PHEA-3%VBABr networks, which

were calculated to be 74±10 kJmol⁻¹ and 71±7 kJmol⁻¹ respectively (Figure S17-18). Interestingly, in both PMSEA-VBABr and PHEA-VBABr materials, networks with higher concentration of bromide anions had faster stress relaxations. Based on this result, we postulate that the attack of bromide anions causes the stress relaxation in these networks. It is also evident from the comparison of relaxation time of PMSEA-5%VBABr and PMSEA-5%VBABr-AS networks at 100 °C (Figure 8). Despite the presence of free amines in PMSEA-5%VBABr-AS networks, the relaxation time was similar to PMSEA-5%VBABr materials, where no free amine is present.

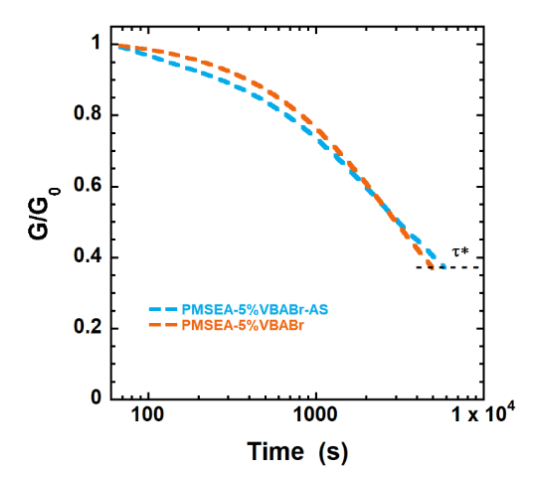


Figure 8. Representative stress relaxation plots of PMSEA-5%VBABr and PMSEA-5%VBABr-AS at 100 °C.

These findings are in agreement with the results of small molecule kinetic study described earlier. To contrast the anilinium bromide-based materials with classically dissociative materials, the stress relaxation behavior of PEA-DA materials was also studied. Figure 9 shows the stress relaxation of PEA-DA networks at elevated temperatures. E_a was calculated to be 103 ±10 kJ/mol from the Arrhenius Plot (Figure S19), which is similar to the values reported in the literature. Interestingly, it is not apparent how to differentiate PHEA-VBABr and PMSEA-VBABr networks with PEA-DA networks based on the qualitative observation of the stress relaxation plots. Although, in

literature, stress relaxation experiments have often been used as a benchmark to characterize flow behavior of vitrimers or vitrimers like materials.⁹

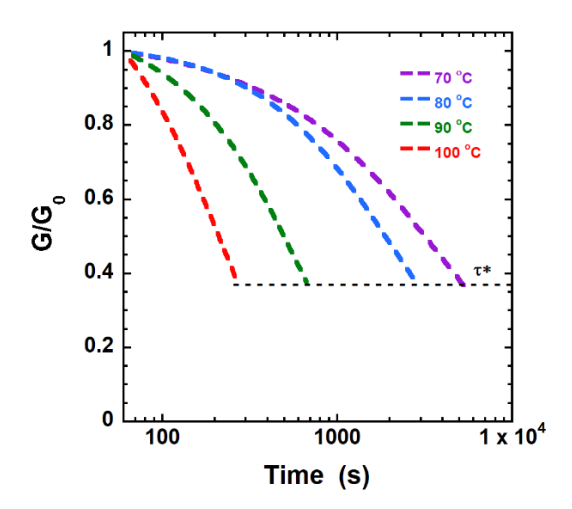


Figure 9. Representative stress relaxation plots of PEA-DA materials.

Temperature sweep experiments on these networks however, provided a clear distinction between the classically dissociative DA based materials and the anilinium bromide-based networks. Figure 10 shows temperature sweep data of all the materials with the change of storage modulus values in respect to temperature. All PHEA-VBABr and PMSEA-VBABr materials showed constant storage moduli values in rubbery plateau region up to 190 °C with G' > G" all the time. This implies no significant decrosslinking has occurred even at >100 °C, above the temperature at which the dissociative exchange in anilinium linkages are activated. A similar result was reported in CANs with dissociative triazolinedione chemistry by the Du Prez group. In contrast, the temperature sweep data of PEA-DA materials show a substantial drop in storage modulus above 100 °C, suggesting a complete dissociation or decrosslinking of DA linkages in the network (Figure 10).

Table 2. Properties of the materials – peak stress, strain at break, Young's Modulus, Healing efficiency at 70 $^{\circ}$ C.

					Healing efficiency		
polymeric materials	peak stress (kPa)	strain at break (mm/mm)	Young's Modulus (kPa)	Tg (°C)	stress (%)	recovered	strain recovered (%)
PHEA-3%VBABr	400 ± 40	3.2 ± 0.2	350 ± 20	8	70±10		65± 5
PHEA-5%VBABr	550 ± 30	$\textbf{2.2} \pm \textbf{0.2}$	620 ± 20	15	40±10		45± 5
PMSEA-3%VBABr	470 ± 40	3.5 ± 0.2	255 ± 15	19	85± 5		8o± 5
PMSEA-5%VBABr	690 ± 30	2.9 ± 0.3	400 ± 30	27	6o± 5		65± 5

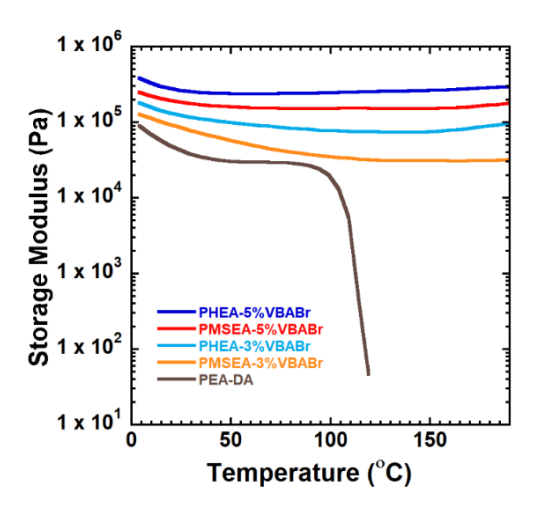


Figure 10. Temperature sweep data of PHEA-VBABr, PMSEA-VBABr, and PEA-DA materials with showing storage modulus values at different temperatures.

This could be attributed to the retro-DA at that temperature as furan-maleimide based DA adducts usually dissociate via retro-DA reaction in around 110 °C. 58,63 However, in the PHEA-VBABr and PSEA-VBABr networks, an essentially constant crosslinked density can be preserved at a wide range of elevated temperatures. To be noted, eventually disappearance of rubbery plateau will be observed in higher temperatures, however, it wasn't observed in our studied temperature range. In all cases, at least two samples were replicated.

Additionally, differential scanning calorimetry (DSC), dynamic mechanical analysis (DMA), infrared spectroscopy (IR), swelling ratio, tensile testing, and rheology were utilized to characterize the properties of the PHEA-VBABr and PMSEA-VBABr materials. IR spectra of PHEA-5%VBABr and PMSEA-5%VBABr materials are given in Figure S20-21. PHEA-3%VBABr and PMSEA-3%VBABr materials also showed similar IR spectrum to PHEA-5%VBABr and PMSEA-5%VBABr materials respectively. DSC curves of these are materials can be found in Figure S22-25 and the glass transition temperature (T_g) were determined to be 8 °C, 15 °C, 19 °C, and 27 °C for PHEA-3%VBABr, PHEA-5%VBABr, PMSEA-3%VBABr, and PMSEA-5%VBABr materials respectively. These values are higher than the homo PHEA (-15 °C) and linear PMSEA (15.7 °C) reported in the literatures^{54,64}, due to crosslinkages and increased rigidity in the networks. Additionally, rheology frequency and strain sweep experiments were also carried out. Frequency sweep experiments provided the storage (G') and loss (G'') moduli values of these materials. All the materials formed a rubbery plateau of G' in low frequency and at higher frequency, these materials showed faster increase in loss modulus than storage modulus with increasing frequency. At oscillation rates exceeding 30 rad/s the materials appear to be approaching the glass transition. These properties are typical of soft and slightly crosslinked materials.^{65,66} All the frequency sweep plots are given in Figure S26-27. In addition, strain sweep experiments showed applied 1% strain is in linear viscoelastic region of PMSEA-5%VBABr material (Figure S28). All other materials also showed similar properties. The stress-strain curves of uncut or virgin PHEA-VBABr and PMSEA-VBABr materials are given in Figure S29-S30. The Young's modulus values of these materials were calculated using Ogden hyper elastic constitutive law. Mechanical properties obtained from tensile testing is given in Table 1, with a trend of increase in peak stress and Young's modulus values but a decrease in strain at break with an increase in crosslinker density

in both PHEA-VBABr and PMSEA-VBABr networks. Both types of materials had highest swelling in water, slight swelling in acetone, and no swelling in hexane (Table S1).

Recycling properties. The recycling ability of these materials were tested by their self-healing or re-healing properties. Here, as no free anilines were incorporated in all of these networks, the healing is surely dictated by the indirect S_N2 pathway i.e. via the bromide attack on benzylic carbon of anilinium salt. Materials were cut and healed at elevated temperature of 70 °C and tensile testing was performed to assess the healing behavior. Figure 11A shows the healing properties of PMSEA-3%VBABr materials. At 16 h healing time, best performing healed materials showed a recovery of 85% in peak stress and 83% in peak strain compared to the uncut materials. Healing times above 16 h shows no significant increase in healing properties. In contrast, PHEA-3%VBABr materials showed moderate healing with best healed material showing peak stress of 70% and peak strain of 65% of uncut materials in 16 h healing time (Figure 11B).

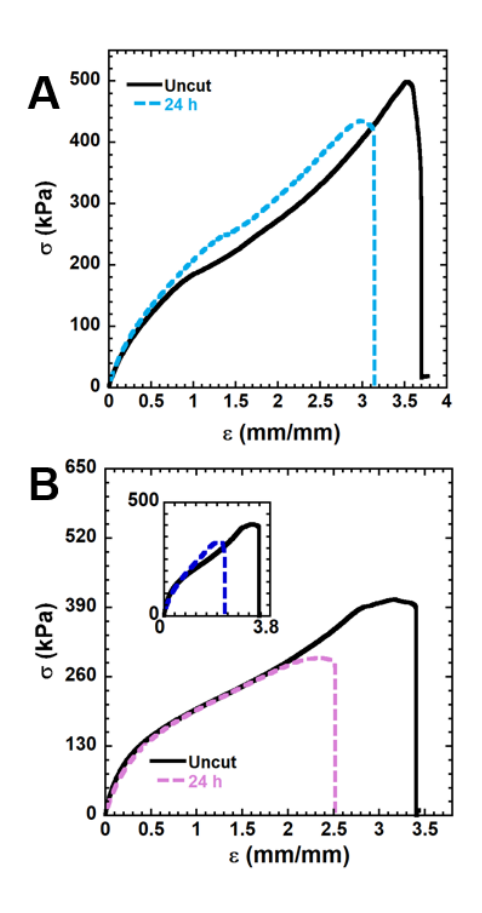


Figure 11. Healing properties of A) PMSEA-3%VBABr and B) PHEA-3%VBABr materials at 70 °C (inset – Healing properties of PHEA-3%VBABr materials in response to 30 s of microwave).

The superior healing properties in PMSEA-VBABr materials again could be attributed to the solvation effect. Both materials with higher crosslinker density showed a decrease in healing properties. Healed PMSEA-5%VBABr materials showed a recovery of 60% in stress and 65% in strain in 16 h (Figure S31A). Healed PHEA-3%VBABr materials on the other hand showed a stress recovery of approximately 40% and a strain recovery of 45% compared to the uncut materials in 16 h time period (Figure S31B). This decrease in healing properties could be attributed to the increase in rigidity or decrease in chain movement in higher crosslinked network. 67,68 In addition to thermal self-healing, microwave assisted self-healing was also observed in PHEA-VBABr materials. When the PHEA-3%VBABr material was heated in a commercially available

microwave just for 30 s, healed materials showed a recovery of 70% in peak stress and 60% in peak strain of uncut materials (Figure 11B inset). Recently, microwave assisted ultra-fast self-healing in CANs has been reported in the literature, where different nanoparticles were used as microwave absorbers. However, the rapid self-healing in PHEA-3%VBABr materials could be attributed to fast heat generated by microwave absorption by the large number of hydroxyl groups in HEA networks and relatively modest temperature requirement for activating anilinium linkages. In addition to healing properties, these materials also showed significant malleability properties. All these materials can be reprocessed and transformed to a new permanent shape at elevated temperatures due to the dynamic bond exchange in the networks. Figure S32 shows the new permanent shape of PMSEA-3%VBABr and PHEA-3%VBABr materials when they were twisted in 360° configuration at 70 °C for 16 h and 24 h respectively.

Mechanical stability. Finally, creep resistance and creep recovery behavior of these materials were appraised. Often dynamic materials show creep deformation under load due to rapid dynamic exchange in ambient conditions. This limits the practicality of using dynamic bonds in materials where resistance to constant load is required. However, PMSEA-5%VBABr material showed creep resistance by reaching a mechanical equilibrium around 20 minutes in room temperature (Figure S33). When the applied stress was removed, PMSEA-5%VBABr material showed a creep recovery of more than 98% in just a 2h time period as shown in Figure S33. Similar creep resistance properties were observed in PMSEA-3%VBABr material, which also showed a creep recovery of around 95% in 2h (Figure S34). Both PHEA-5%VBABr and PHEA-3%VBABr materials also have creep resistance, with 100% and 96% creep recovery respectively (Figure S35). The limited creep in these networks at ambient conditions is attributed to static nature of anilinium linkages at room temperature. The anilinium linkages become dynamic only at elevated

temperatures. The results from creep experiments also act as complementary to stress relaxation study.

Discussion on dissociative DCBs acting like associative DCBs in polymer networks.

In traditional dissociative DCBs like the DA reaction, at lower temperatures (< 70 °C) the formation of DA adduct is favored but at elevated temperatures the thermodynamic equilibrium position significantly shifts from adducts to the reactive species favoring the endothermic but entropically favored reaction, i.e. a significant decrease in equilibrium constant for linker association. The rapid dissociation of DA adducts results in depolymerization in CAN by significant decrease in crosslink density. Additionally, a sudden drop in viscosity profile is observed from viscoelastic solid to viscoelastic liquid. An increase in temperature affects both the kinetics of dissociation and crosslinker density of DA adducts, whereas in a true associative DCBs like TE only the kinetics of exchange increases. 10 Though the dynamic exchange in anilinium adducts follows a dissociative mechanism, there is no sudden drop in crosslinker density, hence a similar rheological profile to associative DCBs is observed. Our small molecular kinetic study shows the equilibrium favoring anilinium adducts instead of the dissociative species at a wide range of elevated temperatures. Also, no significant change in molar concentration of species was observed in studied elevated temperatures. Rowan et al. suggested that a very large Keq is needed for dissociative DCBs to act like vitrimers.⁴⁷ However, in anilinium system, the equilibrium constant was approximately 20 and 3 for MABBr and ABBr respectively. This translates to approximately 82% MABBr or 62% ABBr adducts associated under these conditions. This is certainly not a case where the Keq is so large that an essentially all linkers are associated at all times. A more in-depth study is needed to determine what value of Keq is high enough to maintained an associated network.

The retention of crosslink density could be attributed to rapid decrosslinking and recrosslinking phenomena as reported by Obadia et al.⁴⁸ The small molecule kinetic study showed that both the association and dissociation of anilinium linkages have similar activation energies. Additionally, no measurable entropic change or a balance of species was observed in anilinium system. Most importantly, whereas in traditional dissociative DCBs at elevated temperatures, thermodynamic significantly favors the dissociation of adducts, in anilinium system, the drive towards an increase in dissociation rate is balanced by an equally large drive to reassociation of reactive species to anilinium adducts. Typically, in DA adducts, the equilibrium constant significantly decrease as the temperature increases.^{27,72} This suggest that substituted anilinium salts are unique dissociative systems, due to the measurable and non-trivial fraction of dissociated bond and temperature independence of the fraction of crosslinkers. Although urethanes which can form an isocyanate as a dissociative pathway, the equilibrium constant for adduct formation is so large it cannot be measured, leading to minimal loss of crosslink density as bond exchange occurs, hence why the materials can maintain integrity even upon activation of bond exchange.⁵¹ In contrast, Diels-Alder systems have a substantial change in equilibrium position as bond exchange is promoted. At low temperature Diels-Alder systems, such as furan-maleimide based DA system, temperature dependence of the K_{eq} for the formation of DA adducts is significant and apparent from ΔH value of -157 \pm 14 kJ mol⁻¹. Whereas in case of anilinium adduct MABBr ΔH value is -2.8 \pm 0.2 kJ mol⁻¹ that implies trivial dependence of K_{eq} on temperature. Due to trivial temperature dependency instead of an abrupt drop in viscosity, a gradual and slow drop in viscosity profile was observed. It should be noted that our studied anilinium linkages-based CANs have similar structure and characteristic to MABBr, not ABBr. Further study is to determine whether only MABBr types of networks lead to this retaining of crosslink density. In conclusion, at elevated temperatures a

decrease in crosslinker density is observed in traditional dissociative DCBs such as the DA adducts, however, in anilinium system and associative DCBs crosslinker density remain similar over a range of temperatures. Interestingly, even in DA networks at specific mild temperatures vitrimer like properties can be achieved.⁶² Careful consideration should also be given in characterizing vitrimeric materials. In addition to stress relaxation and temperature sweep experiments, a correlation between kinetics of exchange of a DCB in small molecules and its behavior in CAN should be studied for comprehensive characterization.

Conclusions

In summary, extensive study on small molecular kinetics of exchange in anilinium adducts elucidate the vitrimer like behavior of polymer networks with anilinium linkages. We have shown that exclusively associative exchange in DCBs may not be necessary to achieve vitrimer like properties. Dissociative DCBs where the molar concentration of species is preserved at elevated temperatures, can also be utilized to access vitrimers like behavior. Additionally, the effect of the polarity of main polymer chain on the kinetics of dynamic exchange in anilinium linkages could be used in controlling the viscosity profile of these materials. This report provides a new perspective on associative and dissociative DCBs and their implication in dynamic networks. More effort should be given on studying the thermodynamics of these reaction to properly utilized them in developing advanced functional polymeric materials.

Author Contributions

The manuscript was written through contributions of all authors. All authors have approved the final version of the manuscript.

Funding Sources

This research is supported by the National Science Foundation under Grant No. (DMR-1749730). Acknowledgment is also made to the Donors of the American Chemical Society under Petroleum Research Fund (57243-DNI7) for partial support of this work. Dominik Konkolewicz would also like to acknowledge support from the Robert H. and Nancy J. Blayney Professorship.

Conflicts of Interest

The authors declare no conflicts of interest.

References

- (1) Zhang, W.; Jin, Y.: *Dynamic Covalent Chemistry: Principles, Reactions, and Applications*; John Wiley & Sons, 2017.
- (2) Roy, N.; Bruchmann, B.; Lehn, J. M. DYNAMERS: dynamic polymers as self-healing materials. *Chem. Soc. Rev.* **2015**, *44*, 3786-3807.
- (3) Zhang, Z. P.; Rong, M. Z.; Zhang, M. Q. Polymer engineering based on reversible covalent chemistry: A promising innovative pathway towards new materials and new functionalities. *Prog. Polym. Sci.* **2018**, *80*, 39-93.
- (4) Dahlke, J.; Zechel, S.; Hager, M. D.; Schubert, U. S. How to Design a Self-Healing Polymer: General Concepts of Dynamic Covalent Bonds and Their Application for Intrinsic Healable Materials. *Adv. Mater. Interfaces* **2018**, 1800051.
- (5) Chakma, P.; Konkolewicz, D. Dynamic Covalent Bonds in Polymeric Materials.

 Angew Chem Int Ed Engl 2019, 58, 9682-9695.
- (6) Sun, H.; Kabb, C. P.; Sims, M. B.; Sumerlin, B. S. Architecture-transformable polymers: Reshaping the future of stimuli-responsive polymers. *Prog. Polym. Sci.* **2019**, *89*, 61-75.

- (7) Huynh, T. P.; Sonar, P.; Haick, H. Advanced materials for use in soft self-healing devices. *Adv. Mater.* **2017**, *29*, 1604973.
- (8) Hager, M. D.; Van der Zwaag, S.; Schubert, U. S.: *Self-healing Materials*; Springer, 2016; Vol. 273.
- (9) Scheutz, G. M.; Lessard, J. J.; Sims, M. B.; Sumerlin, B. S. Adaptable Crosslinks in Polymeric Materials: Resolving the Intersection of Thermoplastics and Thermosets. *J. Am. Chem. Soc.* **2019**, *141*, 16181–16196.
- (10) Kloxin, C. J.; Bowman, C. N. Covalent adaptable networks: smart, reconfigurable and responsive network systems. *Chem. Soc. Rev.* **2013**, *42*, 7161-7173.
- (11) Abdallh, M.; Yoshikawa, C.; Hearn, M. T.; Simon, G. P.; Saito, K. Photoreversible Smart Polymers Based on 2π + 2π Cycloaddition Reactions: Nanofilms to Self-Healing Films. *Macromolecules* **2019**, *52*, 2446-2455.
- (12) Chakma, P.; Possarle, L. H. R.; Digby, Z. A.; Zhang, B.; Sparks, J. L.; Konkolewicz, D. Dual stimuli responsive self-healing and malleable materials based on dynamic thiol-Michael chemistry. *Polym. Chem.* **2017**, *8*, 6534-6543.
- (13) Cromwell, O. R.; Chung, J.; Guan, Z. Malleable and self-healing covalent polymer networks through tunable dynamic boronic ester bonds. *J. Am. Chem. Soc.* **2015**, *137*, 6492-6495.
- (14) Foster, E. M.; Lensmeyer, E. E.; Zhang, B.; Chakma, P.; Flum, J. A.; Via, J. J.; Sparks, J. L.; Konkolewicz, D. Effect of Polymer Network Architecture, Enhancing Soft Materials Using Orthogonal Dynamic Bonds in an Interpenetrating Network. *ACS Macro Lett.* **2017**, *6*, 495-499.
- (15) Michal, B. T.; Jaye, C. A.; Spencer, E. J.; Rowan, S. J. Inherently photohealable and thermal shape-memory polydisulfide networks. *ACS Macro Lett.* **2013**, *2*, 694-699.

- (16) Deng, C. C.; Brooks, W. L.; Abboud, K. A.; Sumerlin, B. S. Boronic acid-based hydrogels undergo self-healing at neutral and acidic pH. *ACS Macro Lett.* **2015**, *4*, 220-224.
- (17) Kathan, M.; Kovaříček, P.; Jurissek, C.; Senf, A.; Dallmann, A.; Thünemann, A. F.; Hecht, S. Control of Imine Exchange Kinetics with Photoswitches to Modulate Self-Healing in Polysiloxane Networks by Light Illumination. *Angew. Chem. Int. Ed.* **2016**, *55*, 13882-13886.
- (18) Worrell, B. T.; Mavila, S.; Wang, C.; Kontour, T. M.; Lim, C.-H.; McBride, M. K.; Musgrave, C. B.; Shoemaker, R.; Bowman, C. N. A user's guide to the thiol-thioester exchange in organic media: scope, limitations, and applications in material science. *Polym. Chem.* **2018**, *9*, 4523-4534.
- (19) An, Q.; Wessely, I. D.; Matt, Y.; Hassan, Z.; Bräse, S.; Tsotsalas, M. Recycling and self-healing of dynamic covalent polymer networks with a precisely tuneable crosslinking degree. *Polym Chem.* **2019**, *10*, 672-678.
- (20) Deng, G.; Li, F.; Yu, H.; Liu, F.; Liu, C.; Sun, W.; Jiang, H.; Chen, Y. Dynamic hydrogels with an environmental adaptive self-healing ability and dual responsive sol–gel transitions. *ACS Macro Lett.* **2012**, *1*, 275-279.
- (21) Delahaye, M.; Winne, J. M.; Du Prez, F. E. Internal catalysis in covalent adaptable networks: phthalate monoester transesterification as a versatile dynamic crosslinking chemistry. *J. Am. Chem. Soc.* **2019**, *141*, 15277-15287.
- (22) García, F.; Smulders, M. M. Dynamic covalent polymers. J. Polym. Sci. Part A: Polym. Chem. 2016, 54, 3551-3577.
- (23) Bowman, C. N.; Kloxin, C. J. Covalent adaptable networks: reversible bond structures incorporated in polymer networks. *Angew. Chem. Int. Ed. Engl.* **2012**, *51*, 4272-4274.

- (24) Kwart, H.; King, K. The reverse Diels-Alder or retrodiene reaction. *Chem. Rev.* **1968**, *68*, 415-447.
- (25) Boul, P. J.; Reutenauer, P.; Lehn, J.-M. Reversible Diels– Alder reactions for the generation of dynamic combinatorial libraries. *Org. lett.* **2005**, *7*, 15-18.
- (26) Chen, X.; Dam, M. A.; Ono, K.; Mal, A.; Shen, H.; Nutt, S. R.; Sheran, K.; Wudl, F. A thermally re-mendable cross-linked polymeric material. *Science* **2002**, *295*, 1698-1702.
- (27) Adzima, B. J.; Aguirre, H. A.; Kloxin, C. J.; Scott, T. F.; Bowman, C. N. Rheological and chemical analysis of reverse gelation in a covalently cross-linked Diels– Alder polymer network. *Macromolecules* **2008**, *41*, 9112-9117.
 - (28) Otera, J. Transesterification. *Chem. Rev.* **1993**, *93*, 1449-1470.
- (29) Denissen, W.; Rivero, G.; Nicolaÿ, R.; Leibler, L.; Winne, J. M.; Du Prez, F. E. Vinylogous Urethane Vitrimers. *Adv. Funct. Mater.* **2015**, *25*, 2451-2457.
- (30) Montarnal, D.; Capelot, M.; Tournilhac, F.; Leibler, L. Silica-like malleable materials from permanent organic networks. *Science* **2011**, *334*, 965-968.
- (31) Denissen, W.; Winne, J. M.; Du Prez, F. E. Vitrimers: permanent organic networks with glass-like fluidity. *Chem. Sci.* **2016**, *7*, 30-38.
- (32) Fortman, D. J.; Brutman, J. P.; Cramer, C. J.; Hillmyer, M. A.; Dichtel, W. R. Mechanically activated, catalyst-free polyhydroxyurethane vitrimers. *J. Am. Chem. Soc.* **2015**, *137*, 14019-14022.
- (33) Lessard, J. J.; Garcia, L. F.; Easterling, C. P.; Sims, M. B.; Bentz, K. C.; Arencibia, S.; Savin, D. A.; Sumerlin, B. S. Catalyst-Free Vitrimers from Vinyl Polymers. *Macromolecules* **2019**, *52*, 2105-2111.

- (34) Nishimura, Y.; Chung, J.; Muradyan, H.; Guan, Z. Silyl ether as a robust and thermally stable dynamic covalent motif for malleable polymer design. *J. Am. Chem. Soc.* **2017**, *139*, 14881-14884.
- (35) Zhao, S.; Abu-Omar, M. M. Catechol-Mediated Glycidylation toward Epoxy Vitrimers/Polymers with Tunable Properties. *Macromolecules* **2019**, *52*, 3646-3654.
- (36) Hendriks, B.; Waelkens, J.; Winne, J. M.; Du Prez, F. E. Poly(thioether) Vitrimers via Transalkylation of Trialkylsulfonium Salts. *ACS Macro Lett.* **2017**, *6*, 930-934.
- (37) Feng, Z.; Yu, B.; Hu, J.; Zuo, H.; Li, J.; Sun, H.; Ning, N.; Tian, M.; Zhang, L. Multifunctional Vitrimer-Like Polydimethylsiloxane (PDMS): Recyclable, Self-Healable, and Water-Driven Malleable Covalent Networks Based on Dynamic Imine Bond. *Ind. Eng. Chem. Res.* **2019**, *58*, 1212-1221.
- (38) Snyder, R. L.; Fortman, D. J.; De Hoe, G. X.; Hillmyer, M. A.; Dichtel, W. R. Reprocessable acid-degradable polycarbonate vitrimers. *Macromolecules* **2018**, *51*, 389-397.
- (39) Ishibashi, J. S.; Kalow, J. A. Vitrimeric Silicone Elastomers Enabled by Dynamic Meldrum's Acid-Derived Cross-Links. *ACS Macro Lett.* **2018**, *7*, 482-486.
- (40) Röttger, M.; Domenech, T.; van der Weegen, R.; Breuillac, A.; Nicolaÿ, R.; Leibler, L. High-performance vitrimers from commodity thermoplastics through dioxaborolane metathesis. *Science* **2017**, *356*, 62-65.
- (41) Caffy, F.; Nicolaÿ, R. Transformation of polyethylene into a vitrimer by nitroxide radical coupling of a bis-dioxaborolane. *Polym. Chem.* **2019**, *10*, 3107-3115.
- (42) He, C.; Shi, S.; Wang, D.; Helms, B. A.; Russell, T. P. Poly (Oxime–Ester) Vitrimers with Catalyst-Free Bond Exchange. *J. Am. Chem. Soc.* **2019**, *141*, 13753-13757.

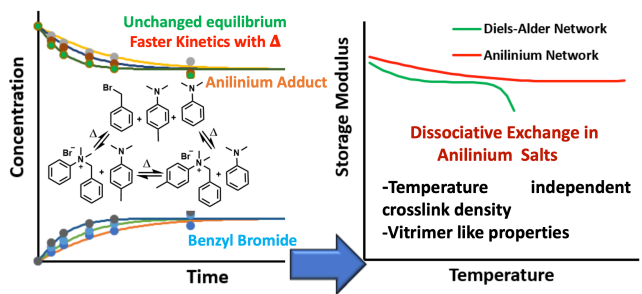
- (43) Tretbar, C. A.; Neal, J. A.; Guan, Z. Direct Silyl Ether Metathesis for Vitrimers with Exceptional Thermal Stability. *J. Am. Chem. Soc.* **2019**, *141*, 16595-16599.
- (44) Saed, M. O.; Gablier, A.; Terentejv, E. M. Liquid Crystalline Vitrimers with Full or Partial Boronic-Ester Bond Exchange. *Adv. Funct. Mater.* **2020**, *30*, 1906458.
- (45) Chakma, P.; Digby, Z. A.; Shulman, M. P.; Kuhn, L. R.; Morley, C. N.; Sparks, J. L.; Konkolewicz, D. Anilinium Salts in Polymer Networks for Materials with Mechanical Stability and Mild Thermally Induced Dynamic Properties. *ACS Macro Lett.* **2019**, *8*, 95-100.
- (46) Kulchat, S.; Lehn, J. M. Dynamic Covalent Chemistry of Nucleophilic Substitution Component Exchange of Quaternary Ammonium Salts. *Chem. Asian J.* **2015**, *10*, 2484-2496.
- (47) Zhang, L.; Rowan, S. J. Effect of Sterics and Degree of Cross-Linking on the Mechanical Properties of Dynamic Poly (alkylurea–urethane) Networks. *Macromolecules* **2017**, 50, 5051-5060.
- (48) Obadia, M. M.; Jourdain, A.; Cassagnau, P.; Montarnal, D.; Drockenmuller, E. Tuning the Viscosity Profile of Ionic Vitrimers Incorporating 1, 2, 3-Triazolium Cross-Links. *Adv. Func. Mater.* **2017**, *27*, 1703258.
- (49) Obadia, M. M.; Mudraboyina, B. P.; Serghei, A.; Montarnal, D.; Drockenmuller, E. Reprocessing and recycling of highly cross-linked ion-conducting networks through transalkylation exchanges of C–N bonds. *J. Am. Chem. Soc.* **2015**, *137*, 6078-6083.
- (50) Van Herck, N.; Du Prez, F. E. Fast healing of polyurethane thermosets using reversible triazolinedione chemistry and shape-memory. *Macromolecules* **2018**, *51*, 3405-3414.
- (51) Brutman, J. P.; Fortman, D. J.; De Hoe, G. X.; Dichtel, W. R.; Hillmyer, M. A. Mechanistic Study of Stress Relaxation in Urethane-Containing Polymer Networks. *J. Phys. Chem. B* **2019**, *123*, 1432-1441.

- (52) Shergold, O. A.; Fleck, N. A.; Radford, D. The uniaxial stress versus strain response of pig skin and silicone rubber at low and high strain rates. *Int. J. Impact Eng.* **2006**, *32*, 1384-1402.
- (53) Li, S.; Chung, H. S.; Simakova, A.; Wang, Z.; Park, S.; Fu, L.; Cohen-Karni, D.; Averick, S.; Matyjaszewski, K. Biocompatible polymeric analogues of DMSO prepared by atom transfer radical polymerization. *Biomacromolecules* **2017**, *18*, 475-482.
- (54) Mackenzie, M. C.; Shrivats, A. R.; Konkolewicz, D.; Averick, S. E.; McDermott, M. C.; Hollinger, J. O.; Matyjaszewski, K. Synthesis of poly (meth) acrylates with thioether and tertiary sulfonium groups by ARGET ATRP and their use as siRNA delivery agents. *Biomacromolecules* **2014**, *16*, 236-245.
- (55) Mäsing, F.; Mardyukov, A.; Doerenkamp, C.; Eckert, H.; Malkus, U.; Nüsse, H.; Klingauf, J.; Studer, A. Controlled Light-Mediated Preparation of Gold Nanoparticles by a Norrish Type I Reaction of Photoactive Polymers. *Angew. Chem., Int. Ed.* **2015**, *54*, 12612-12617.
- (56) Hisey, B.; Buddingh, J. V.; Gillies, E. R.; Ragogna, P. J. Effect of Counterions on the Self-Assembly of Polystyrene–Polyphosphonium Block Copolymers. *Langmuir* **2017**, *33*, 14738-14747.
- (57) Kulchat, S.; Lehn, J. M. Dynamic Covalent Chemistry of Nucleophilic Substitution Component Exchange of Quaternary Ammonium Salts. *Chem Asian J* **2015**, *10*, 2484-2496.
- (58) McElhanon, J. R.; Wheeler, D. R. Thermally responsive dendrons and dendrimers based on reversible furan-maleimide Diels- Alder adducts. *Org. lett.* **2001**, *3*, 2681-2683.
- (59) Parker, A. J. Protic-dipolar aprotic solvent effects on rates of bimolecular reactions. *Chem. Rev.* **1969**, *69*, 1-32.

- (60) Alemán, C.; Maseras, F.; Lledós, A.; Duran, M.; Bertrán, J. Analysis of solvent effect on SN2 reactions by different theoretical models. *J. Phys. Org. Chem.* **1989**, *2*, 611-622.
- (61) Parker, A.; Mayer, U.; Schmid, R.; Gutmann, V. Correlation of solvent effects on rates of solvolysis and SN2 reactions. *J. Org. Chem.* **1978**, *43*, 1843-1854.
- (62) Kuang, X.; Liu, G.; Dong, X.; Wang, D. Correlation between stress relaxation dynamics and thermochemistry for covalent adaptive networks polymers. *Mater. Chem. Front.* **2017**, *1*, 111-118.
- (63) Bose, R. K.; Kötteritzsch, J.; Garcia, S. J.; Hager, M. D.; Schubert, U. S.; van der Zwaag, S. A rheological and spectroscopic study on the kinetics of self-healing in a single-component diels–alder copolymer and its underlying chemical reaction. *J. Polym. Sci. Part A: Polym. Chem.* **2014**, *52*, 1669-1675.
- (64) Vargün, E.; Usanmaz, A. Polymerization of 2-hydroxyethyl acrylate in bulk and solution by chemical initiator and by ATRP method. *J. Polym. Sci. Part A: Polym. Chem.* **2005**, 43, 3957-3965.
- (65) Cordier, P.; Tournilhac, F.; Soulie-Ziakovic, C.; Leibler, L. Self-healing and thermoreversible rubber from supramolecular assembly. *Nature* **2008**, *451*, 977-980.
- (66) Ahmadi, M.; Pioge, S.; Fustin, C.-A.; Gohy, J.-F.; Van Ruymbeke, E. Closer insight into the structure of moderate to densely branched comb polymers by combining modelling and linear rheological measurements. *Soft matter* **2017**, *13*, 1063-1073.
- (67) Garcia, S. J. Effect of polymer architecture on the intrinsic self-healing character of polymers. *Eur. Polym. J.* **2014**, *53*, 118-125.

- (68) Chakma, P.; Digby, Z.; Via, J.; Shulman, M.; Sparks, J.; Konkolewicz, D. Tuning Thermoresponsive Network Materials through Macromolecular Architecture and Dynamic Thiol-Michael Chemistry. *Polym. Chem.* **2018**, *9*, 4744-4756.
- (69) Solouki Bonab, V.; Karimkhani, V.; Manas-Zloczower, I. Ultra-Fast Microwave Assisted Self-Healing of Covalent Adaptive Polyurethane Networks with Carbon Nanotubes. *Macromol. Mater. Eng.* **2019**, *304*, 1800405.
- (70) Menon, A. V.; Madras, G.; Bose, S. Ultrafast self-healable interfaces in polyurethane nanocomposites designed using diels-alder "click" as an efficient microwave absorber. *ACS Omega* **2018**, *3*, 1137-1146.
- (71) Hart, L. R.; Harries, J. L.; Greenland, B. W.; Colquhoun, H. M.; Hayes, W. Healable supramolecular polymers. *Polym. Chem.* **2013**, *4*, 4860-4870.
- (72) Buonerba, A.; Lapenta, R.; Ortega Sánchez, S.; Capacchione, C.; Milione, S.; Grassi, A. A Comprehensive Depiction of the Furan-Maleimide Coupling via Kinetic and Thermodynamic Investigations of the Diels-Alder Reaction of Poly (styrene–co-2-vinylfuran) with Maleimides. *ChemistrySelect* **2017**, *2*, 1605-1612.

Graphical Abstract for Publication



Model Studies Explain and Guide Materials